Aerosol and Air Quality Research, 17: 2381–2389, 2017

ISSN: 1680-8584 print / 2071-1409 online
doi: 10.4209/aaqr.2016.08.0372

Chemical Analysis of Particulate Matter in the Harvest Period in an Agricultural Region of Eastern China

Danni Liang, Xian Ma, Jinsheng Zhang, Zejun Liu, Jianhui Wu*, Yinchang Feng, Yufen Zhang

State Environmental Protection Key Laboratory of Urban Ambient Air Particulate Matter Pollution Prevention and Control, College of Environmental Science and Engineering, Nankai University, Tianjin 300071, China

ABSTRACT

$PM_{2.5}$ samples were collected for August 13–22 (non-harvest period, NHP) and for October 21–31 (harvest period, HP) in 2014 from an agricultural region of Eastern China. The samples were subsequently analysed to determine mass concentrations and fractions of elements, water-soluble ions and carbon components. Online datasets (SO_2, NO_2, O_3, CO, PM_{10} and $PM_{2.5}$) and meteorological conditions were synchronously monitored. The average mass concentrations of $PM_{2.5}$ during the HP and NHP were respectively 108.3 and 62.6 μg m^{-3}. Compared with the mass concentrations of organic carbon (OC), Cl^-, NO_3^- and K^+ during the NHP, those during the HP were significantly increased. Moreover, the mass fractions of OC, elemental carbon (EC), Cl^- and K^+ during the HP were respectively 1.6, 1.3, 3.2 and 1.3 times of those during the NHP. SO_4^{2-}, NO_3^-, and OC were the major chemical components in $PM_{2.5}$ during the HP, indicating that biomass burning and secondary transformation may be two major sources of $PM_{2.5}$ during the HP. The K^+/Cl^- value in $PM_{2.5}$ during the HP was lower than 1, indicating that maize straws were the crop residues in the study area. Although the sulphur and nitrogen oxidation ratios during the HP were lower than during the NHP, the effects of the secondary transformation on particles cannot be ignored during the HP. Biomass burning yielded a 58% OC concentration during the HP.

***Keywords*:** Agricultural region; Harvest period; $PM_{2.5}$; Crop residue burning; Characteristics.

INTRODUCTION

With the increasing demand for more favourable air quality in recent years, $PM_{2.5}$ has drawn considerable attention (Hu *et al*., 2011; Zheng *et al*., 2014; Sun *et al.*, 2016); $PM_{2.5}$ is a type of particulate matter with an aerodynamic diameter of less than 2.5 μm. As an atmospheric pollutant, $PM_{2.5}$ can cause visibility degradation, affect surface solar radiation and damage to human health (Dockery *et al.*, 1993; Watson, 2002; Yuan *et al.*, 2006; Duan *et al.*, 2013; Zhang *et al.*, 2013).

In China, opening burning of crop residue has been reported as the principal source of $PM_{2.5}$, which also causes heavy regional haze pollution (Huang *et al.*, 2013; Cheng *et al*., 2014). More than 1.8 billion hectares of farmland in China is used for food production (Luo *et al*., 2016), and large quantities of crop residue are burned in farmlands during the harvest period (HP) each year (Andreae and Merlet, 2001; Cao *et al.*, 2008; Jain *et al.*, 2014). In China, the harvest period includes two periods, summer period (from late May to early June) and autumn period (from late October to early November) (Huang *et al.*, 2013; Zhang *et al.*, 2017). This human activity has increased the emissions of harmful gases and $PM_{2.5}$, which aggravates air pollution, affects the ground radiation balance, and damages human health during the harvest season. Crop residue burning is a type of biomass burning, Street *et al.* (2003) estimated that Asia burned 730 Tg of biomass in 2000, among which, 250 Tg biomass was released by crop residue burning. Therefore, crop residue burning is a critical source of $PM_{2.5}$, and it is essential that the effects of crop residue burning on air quality and the characteristics of pollutants during the HP are determined.

Studies have determined the source apportionment of particulates in numerous large cities, such as Beijing (Liu *et al.*, 2014), Shanghai (Hu *et al.*, 2014), and Guangzhou (Cui *et al.*, 2015), and biomass burning has markedly contributed to $PM_{2.5}$ and increased the mass concentrations of K^+, Cl^- and carbon components (Li *et al.*, 2007; Lin *et al.*, 2010; Zhang *et al.*, 2015). Farmlands in the aforementioned developed cities are mainly located in the suburbs or surrounding cities, therefore, the effects of crop residue burning on air quality are small in these cities. Hence, we must select an agricultural city which burns crop residues during the harvest season to determine how crop residue burning affects atmospheric quality.

* Corresponding author.
Tel.: 1-392-077-9769; Fax: 0-222-350-3397
E-mail address: envwujh@nankai.edu.cn

As the Ministry of Environmental Protection of the People's Republic of China reported, for late October in 2014, the Shandong province ranked third through the country according the numbers of straw burning fire and fifth according to the intensity of straw burning fire. We chose Heze City as the study area, which is a developing city located in the southwest of the Shandong province (34°39′–35°52′N, 114°45′–116°25′E). It is a predominantly agricultural city whose farmlands accounts for 68.3% of the city's total area. October is the maize harvest period for Heze, and large quantities of maize residues are burned during the HP. We selected this city as the study area and analysed the following factors: (1) pollutant characteristics during the HP, (2) chemical component characteristics of $PM_{2.5}$ during the HP, (3) the differences in the chemical components between HP and the non-harvest period (NHP), and (4) the effects of crop residue burning on the atmosphere.

METHOD

Sampling

Fig. 1 and Table 1 show the location and surroundings of the sampling sites. $PM_{2.5}$ samples were collected for October to 21–31 in 2014 during the HP, and for August 13–22 in 2014 during a NHP for comparison. Gaseous pollutant concentrations and meteorological conditions were monitored synchronously at the sampling stations. The difference in the pollution sources for HP and NHP depend on agricultural emission conditions, these include crop residue burning emissions for HP and biogenic emissions for NHP. During the NHP, the main sources of particles are combustion, industrial emissions, automobile exhaust and flowing dust. For HP, crop residue burning emissions is the main source of $PM_{2.5}$, the contribution of other sources (e.g., combustion, industrial emissions, automobile exhaust and flowing dust) to $PM_{2.5}$ is low.

Two types of filter were used to collect particulate matters: Teflon filters (90 mm diameter) were used to analyse elements, and quartz filters (90 mm diameter) were used to analyse ions and carbon. The pre-treatment for filters was as follows: the Teflon and quartz filters were respectively baked in ovens at 60°C and 400–500°C for at least two hours; after baked, all blank filters were kept in silica gel desiccators for at least three days before being weighed. An over one hundred thousandth (1/100000) scale (Mettler Toledo AX205) was used to weigh the filters before and after sampling. Two pre-calibrated samplers (TH-150, Wuhan Tianhong Intelligence Instrument Facility, China) collected $PM_{2.5}$ samples at each site via equipped Teflon

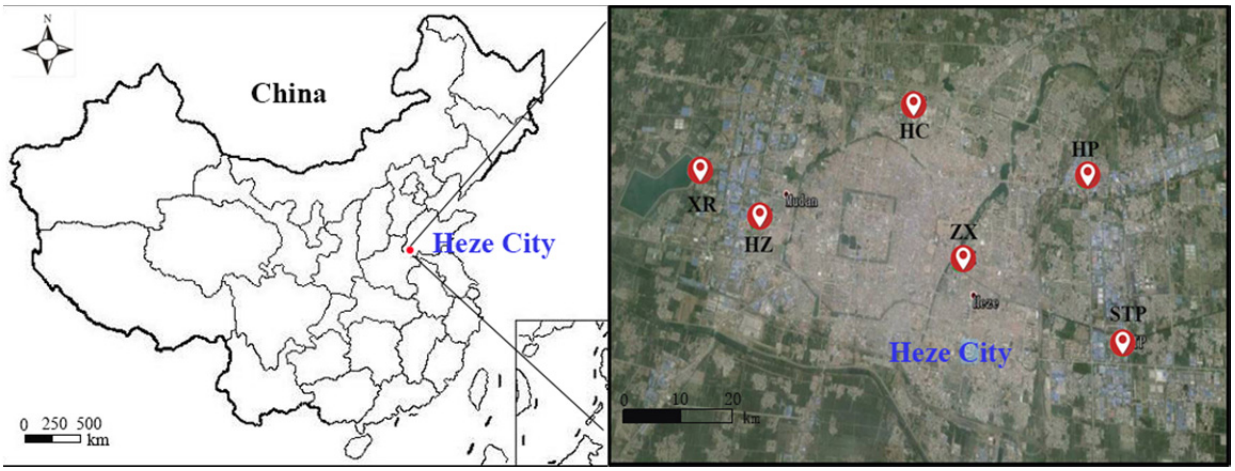

Fig. 1. Sampling sites in Heze City.

Table 1. Location and surroundings of the sampling sites.

Sampling sites	Location	Surroundings
Sewage Treatment Plant (STP)	35°13.35 N 115°31.60 E	power plant, chemical plant, pharmaceutical factory
High-tech Zone (HZ)	35°14.64 N 115°24.46 E	residential area, traffic arteries
Municipal Political Consultative Conference (ZX)	35°14.25 N 115°28.48 E	residential area, traffic arteries
Heze Colledge (HG)	35°16.16 N 115°27.60 E	school, residential area, traffic arteries
West Reservoir (XR)	35°15.21 N 115°23.17 E	farmland, farmstead, cattle farm
Huarun Pharmaceutical Factory (HP)	35°15.38 N 115°30.95 E	traffic arteries, pharmaceutical factory

filters or quartz filters. All samplers were collected at a flow rate of 100 L min^{-1} for at least 20 hours during a 24 h time cycle. Before analysis, all filters were reserved in a refrigerator (4°C).

Quality assurance and quality control (QA/QC) in the sampling process of $PM_{2.5}$ mainly included: (1) The flow of each sampler was calibrated every day to eliminate system errors; (2) all of the samplers at each site were started at the same time every day; (3) all of the filters were ensured to maintain integrity at every step of sampling; (4) the fraction of the parallel samplers aimed to be 10% of the total, and the relative standard deviations of the parallel samples were equal to or less than 20%.

Chemical Analysis

After sampling and weighing, each sample was analysed for chemical components including elements (Na, Mg, Al, Si, K, Ca, Ti, V, Cr, Fe, Mn, Zn, Ni, Cu and Pb), organic carbon (OC), elemental carbon (EC), and water-soluble inorganic ions (Na^+, Mg^{2+}, Ca^{2+}, K^+, NH_4^+, F^-, Cl^-, NO_3^- and SO_4^{2-}).

Elements were analysed using inductively coupled plasma mass spectrometry [ICP 9000(N+M), USA]. A quarter of each Teflon filter was cut into fragments and treated with a mixture of 4 mL HNO_3, 2 mL HCl and 1 mL H_2O_2. The sample and acid mixtures were heated with an electric stove and evaporated until 3 mL of residual remained. When cooled to room temperature, the sample was transferred to a test tube and diluted with deionised water. Si and Al were analysed using an alkali solution was used, and the treatment procedure was the same. Reagent blanks were tested, and the test results were under the detection limits. Two blank samples was analysed for every 20 samples to ensure relative standard deviation of element contents between the two blank samples was less than 20%. The limits of detection for Na, Mg, Al, Si, K, Ca, Ti, V, Cr, Mn, Fe, Ni, Cu, Zn and Pb were 0.0002, 0.00005, 0.0002, 0.005, 0.004, 0.0005, 0.005, 0.003, 0.004, 0.0005, 0.002, 0.009, 0.002, 0.005 and 0.03 μg mL^{-1}.

OC and EC were determined by an OC/EC analyser (Atmoslytic Inc. DRI2001A, USA) using a punch of each quartz filter of area 0.558 cm^2. An IMPROVE thermal/optical transmittance method was applied to measure the concentrations of OC and EC. The carbon analysis process contained seven steps of heating programs, including 140°C (OC1), 280°C (OC2), 480°C (OC3), 580°C (OC4), 580°C (EC1), 740°C (EC2) and 840°C (EC3). When each sample was analysed, we could determine the concentrations of OC1, OC2, OC3, OC4, EC1, EC2, EC3 and pyrolysis carbon (OPC). IMPROVE defines OC and EC as follows:

$$OC = OC1 + OC2 + OC3 + OC4 + OPC \quad (1)$$

$$EC = EC1 + EC + EC3 - OPC \quad (2)$$

The respective detection limits of OC and EC were 0.45 and 0.06 μg cm^{-2}. A repeat sample was analysed for every 10 samples to ensure that the instrument precision error was less than 2%. The analyser was calibrated every day before and after the analysis.

The water-soluble inorganic ions were analysed via ionic chromatography (IC, Dionex ICS–900, USA). A quarter of the quartz filter was extracted into 5 mL with deionized water in an ultrasonic bath (GT sonic, GT-2120QTS, China) for 15 min, with a frequency of 40Hz. Then, 1 mL of supernatant solution was extracted using a syringe equipped with a disposable filter head (with 0.22 μm pore size). Finally, the supernatant solution was injected into the ion chromatograph. Field blanks were tested to calibrate the concentrations of ionic species, and the test results were under the detection limits. The standard solutions were detected three times prior to analysis, and low relative standard deviations were observed. The respective detection limits of Na^+, Mg^{2+}, Ca^{2+}, K^+, NH_4^+, F^-, Cl^-, NO_3^- and SO_4^{2-} were 0.004, 0.006, 0.007, 0.007, 0.017, 0.009, 0.01, 0.07 and 0.05 μg m^{-3}.

RESULTS AND DISCUSSION

Concentrations of Gaseous Pollutants and Particulate Matters

Table 2 shows the mass concentrations of the six pollutants and meteorological conditions during the NHP and HP. The relative humidity and wind speed showed minor differences between the NHP and HP, and temperature during the HP was 8.9°C lower than during the NHP (Table 2). Temperature during the NHP and HP were above 16°C, NHP and HP were in a warmer season in a year, usually diffusion condition in a warmer season is better.

The mass concentration of SO_2 during the HP was 48.7 μg m^{-3}, which was 2.3 times that during the NHP. The mass concentrations of NO_2 and CO during the HP were respectively 53.7 μg m^{-3} and 1.7 mg m^{-3}, which were 1.6 and 1.3-fold higher than those during the NHP. The respective concentrations of PM_{10} and $PM_{2.5}$ during the HP were 181.5 and 108.3 μg m^{-3}, which were 1.9 and 1.7-fold higher than during the NHP. The mass concentration of O_3 was markedly higher during the NHP (84.7 μg m^{-3}) because of the stronger sunlight and higher temperatures. This may

Table 2. Mass concentrations of pollutants and meteorological conditions in Heze City during the study period.

Period	SO_2 (μg m^{-3})	NO_2 (μg m^{-3})	CO (mg m^{-3})	O_3 (μg m^{-3})	PM_{10} (μg m^{-3})
NHP	21.5 ± 8.0	34.0 ± 7.8	1.3 ± 0.2	84.7 ± 13.5	96.7 ± 28.2
HP	48.1 ± 19.0	53.7 ± 10.0	1.7 ± 0.4	35.5 ± 20.4	181.5 ± 36.9
Period	$PM_{2.5}$ (μg m^{-3})	T (°C)	RH (%)	WS (m s^{-1})	
NHP	62.6 ± 25.5	25.3 ± 1.6	79.1 ± 5.6	1.3 ± 0.3	
HP	108.3 ± 34.3	16.5 ± 2.3	72.7 ± 9.1	1.8 ± 0.5	

T, temperature; RH, relative humidity; WS, wind speed.

also account for the mass concentrations of SO_2 and NO_2 being lower during the NHP than during the HP. During the NHP, strong sunlight facilitated photochemical reactions, and more SO_2 and NO_2 were respectively transformed into SO_4^{2-} and NO_3^- (Khoder, 2002; Liu *et al*., 2011). Briefly, the mass concentrations of particulate matter and gaseous pollutants markedly increased during the HP, whereas the mass concentration of O_3 decreased. The present findings are in concordance with the studies conducted by Andreae and Merlet (2001) and Cheng *et al.* (2013), who reported that biomass burning, including crop residue burning, contributed to large quantities of particles and trace gases.

Chemical Components Characteristics in $PM_{2.5}$

The mass concentrations of major chemical components in $PM_{2.5}$ during the NHP are shown in Fig. (2(a)). Among the major chemical components, the mass concentration of SO_4^{2-} was highest (23.8 μg m^{-3}). NO_3^-, OC, crustal elements (Al, Si and Ca), NH_4^+, and EC were present in moderate concentrations, with respective mass concentrations of 8.7, 7.1, 6.9, 4.8 and 3.3 μg m^{-3}. Among the water-soluble ions, the respective mass concentrations of Cl^- and K^+ were lower, at 1.1 and 0.9 μg m^{-3}.

The mass concentrations of the major chemical components in $PM_{2.5}$ during the HP are shown in Fig. 2(b). The major components were SO_4^{2-}, NO_3^- and OC, at respective mass concentrations of 21.5, 20.8, and 18.4 μg m^{-3}. The respective mass concentrations of NH_4^+, EC, and Cl^- were moderate, at 8.7, 6.7, and 5.7 μg m^{-3}. The mass concentration crustal elements were similar to those of EC, which was approximately 3.5-fold higher than that of K^+. Compared with the mass concentrations of OC, Cl^-, and NO_3^- during the NHP, those during the HP were significantly increased. Although the mass concentrations of K^+ during the NHP and HP were lower than 2 μg m^{-3}, the mass concentration of K^+ during the HP was 2.1-fold higher than during the NHP.

Fig. 3(a) shows the mass fractions of different chemical components detected during the NHP. The mass fraction of SO_4^{2-} was highest (40.4%), followed by that of NO_3^- (14.6%). SO_4^{2-} and NO_3^- are respectively markers of secondary SO_4^{2-} and secondary NO_3^- (Song *et al.*, 2006; Lestari *et al.*, 2009), and their high mass fractions indicate that the secondary transformations of SO_2 and NO_x are crucial sources of $PM_{2.5}$ during the NHP. Considering carbon components, the mass fractions of OC and EC were respectively 12.1% and 5.5%. The mass fraction of crustal elements was 11.6%, and NH_4^+ (mass fraction, 8.0%) ranked third among the water-soluble ions. The mass fractions of Cl^- (1.9%) and K^+ (1.6%) were similar.

Fig. 3(b) shows the mass fractions of different chemical components detected during the HP. The mass fractions of SO_4^{2-} and NO_3^- exceeded 20%, and the mass fraction of OC was 19.6%, these components accounted for more than half of the detected chemical components. NH_4^+ (mass fraction, 9.3%) ranked third among the water-soluble ions. Furthermore, the mass fraction of the marker for coal combustion and wheat straw burning (Cl^-) (Zheng *et al.*, 2005a; Song *et al.*, 2006; Li *et al.,* 2007) was 6.0%. The mass fraction of K^+ was 2.1%, K^+ was the tracer of biomass burning (Cheng *et al.*, 2013; Sopittaporn *et al.*, 2013). The mass fractions of both EC and the crustal elements were approximately 7%. Therefore, biomass burning and the secondary transformation of SO_2 and NO_x may be concluded as being two major sources of $PM_{2.5}$ during the HP in Heze City. Compared with the mass fractions of OC, EC, Cl^-, and K^+ during the NHP, those during the HP were markedly increased, and were respectively 1.6, 1.3, 3.2, and 1.3-fold higher than those during the NHP.

Crop residues have varying emission characteristics;

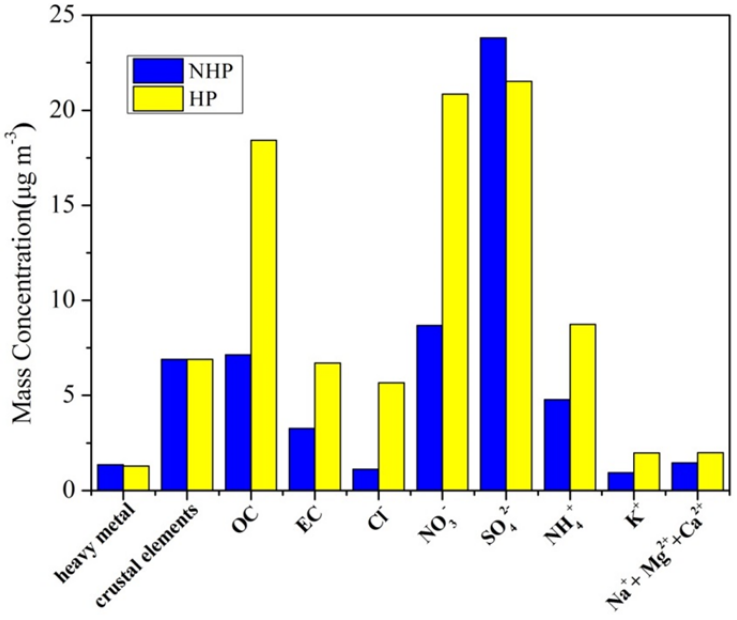

Fig. 2. Mass concentrations of major chemical components in $PM_{2.5}$ during the NHP and HP (heavy metals: As, Cd, Cr, Cu, Fe, Mn, Ni, Pb, V, and Zn; crustal elements: Al, Si, and Ca).

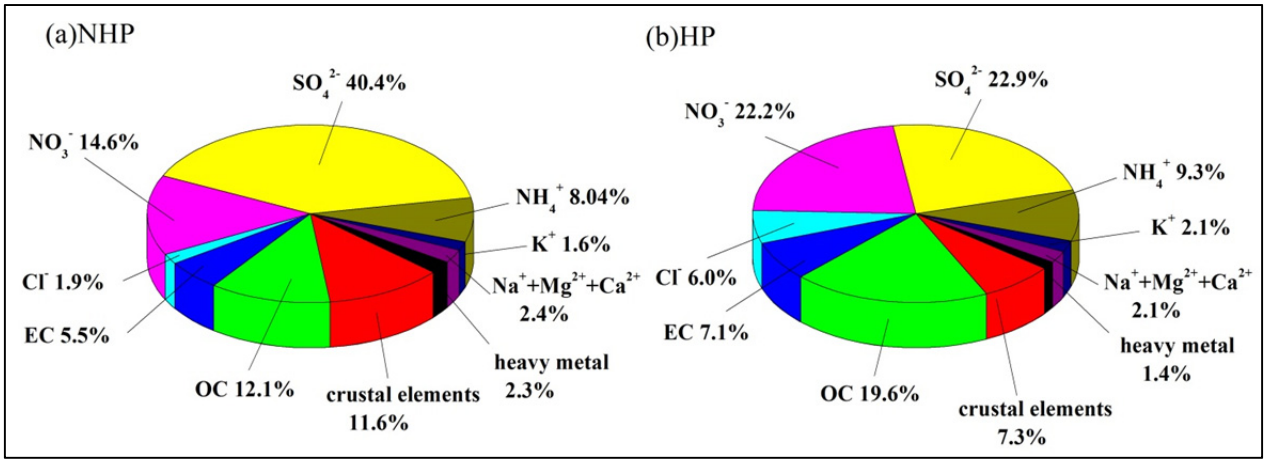

Fig. 3. Mass fractions of different chemical components in the detected components during the NHP and HP (heavy metals: As, Cd, Cr, Cu, Fe, Mn, Ni, Pb, V, and Zn; crustal elements: Al, Si, and Ca).

Table 3 shows the percentages of OC, EC, K^+ and Cl^- in $PM_{2.5}$ of different kinds of crop residues. We can conclude that the K^+/Cl^- values vary in crop residues. The K^+/Cl^- values for maize straws were lower than 1 (Turn *et al.*, 1997; Li *et al.*, 2007), but that for wheat straws was higher than 1 (Turn *et al.*, 1997; Hays *et al.*, 2008). This value ranged 0.6–1.0 for rice straws (Turn *et al.*, 1997; Hays *et al.*, 2008). The K^+/Cl^- values for sugarcane straw were similar to those for rice straws, in the range 0.6–1.0 (Turn *et al.*, 1997). In our study, the K^+/Cl^- value of $PM_{2.5}$ was 0.4, which is lower than 1, and maize harvesting in Heze City was performed in October. Therefore, maize straws were the crop residues in Heze City during the HP.

Secondary Inorganic Ions

As previously mentioned, we concluded that SO_4^{2-} and NO_3^- play crucial roles in $PM_{2.5}$, and they are commonly called secondary inorganic ions. Therefore, it is vital to focus on secondary inorganic ions.

Secondary inorganic ions (SO_4^{2-}, NO_3^-, and NH_4^+) are crucial components of fine particle matter (Mather *et al.*, 2003; Eliana *et al.*, 2014) and play vital roles in visibility reduction, global radiation budgets, regional haze pollution, and human health (Haywood *et al.*, 2008; Liu *et al.*, 2008; Wang *et al.*, 2012). Ammonia vapour can react with acidic gas or condense on the surface of acidic particles and accumulate in droplets, subsequently generating particulate NH_4^+ (Hong *et al.*, 1999). The correlation between NH_4^+ and SO_4^{2-} in $PM_{2.5}$ can suggest their presence in particulate matter (Wang *et al.*, 2015).

Fig. 4 shows that when the molar ratio of NH_4^+ to SO_4^{2-} for $PM_{2.5}$ was 2, NH_4^+ and SO_4^{2-} existed in the form of $(NH_4)_2SO_4$ (Possanzini *et al.*, 1999; Deng *et al.*, 2010). When the molar ratio of NH_4^+ to SO_4^{2-} for $PM_{2.5}$ was 1, they existed in the form NH_4HSO_4 (Deng *et al.*, 2010). The average molar concentration ratio of NH_4^+ to SO_4^{2-} for $PM_{2.5}$ during the HP was 1.8, which was close to 2, indicating that NH_4^+ and SO_4^{2-} mainly existed in the form $(NH_4)_2SO_4$ in $PM_{2.5}$. Moreover, the average molar concentration ratio of NH_4^+ to SO_4^{2-} for $PM_{2.5}$ during the NHP was 1.0, which was close to 1, indicating that NH_4^+ could not sufficiently neutralize SO_4^{2-} during the NHP and may exist in the atmosphere in the form of NH_4HSO_4.

As the primary water-soluble ions in atmospheric particulate matter, SO_4^{2-} and NO_3^- are mainly formed by SO_2 and NO_x, respectively, through a series of photochemical reactions (Duan *et al.*, 2003). We used the sulphur oxidation ratio (SOR) and nitrogen oxidation ratio (NOR) to represent the respective transformation ratios of SO_2 and NO_2 to estimate the respective transformation of SO_2 and NO_x to SO_4^{2-} and NO_3^-. Higher SOR and NOR were associated with a stronger oxidation capacity in the atmosphere, and more gaseous pollutants transformed into SO_4^{2-} and NO_3^- in the particulate matter (Grosjean and Seinfeld, 1989;

Table 3. Chemical composition of $PM_{2.5}$ emitted from different crop residue fires (% $PM_{2.5}$).

	K^+	Cl^-	K^+/Cl^-	References
Maize straws	9	23	0.4	Li *et al.*, 2007
Maize straws	14	26	0.5	Turn *et al.*, 1997
Maize straws	10	14	0.7	Li *et al.*, 2007
Wheat straws	25	24	1.0	Hays *et al.*, 2008
Wheat straws	15	5	3.0	Turn *et al.*, 1997
Rice straws	1	1	1.0	Hays *et al.*, 2008
Rice straws	15	27	0.6	Turn *et al.*, 1997
Sugarcane straws	12	18	0.7	Turn *et al.*, 1997
	2	5.7	0.4	This study

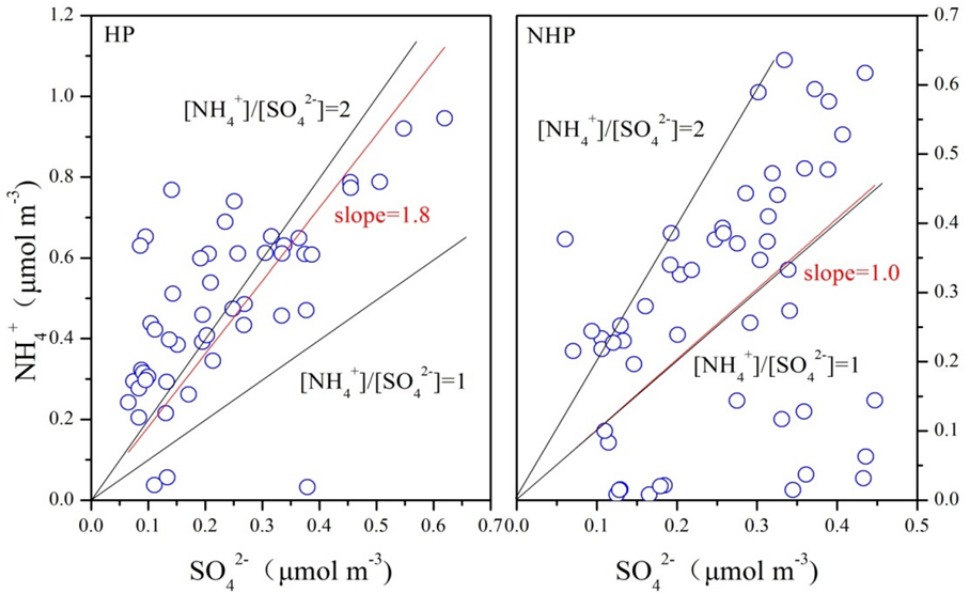

Fig. 4. Molar ratio of NH_4^+ to SO_4^{2-} for $PM_{2.5}$.

Wen *et al.*, 2007). The formulae for SOR and NOR are as follows (Grosjean and Friedlander, 1975; Kadowaki, 1986; Ohta and Okita, 1990):

$$SOR = [SO_4^{2-}]/([SO_4^{2-}] + [SO_2]) \quad (1)$$

$$NOR = [NO_3^-]/([NO_3^-] + [NO_2]) \quad (2)$$

where $[SO_4^{2-}]$ and $[SO_2]$ respectively represent the mass concentrations (μg S m^{-3}) of SO_4^{2-} and SO_2, and $[NO_3^-]$ and $[NO_2]$ respectively represent the mass concentrations (μg N m^{-3}) of NO_3^- and NO_2 (Kadowaki, 1986; Grosjean and Friedlander, 1975; Ohta and Okita, 1990).

The SORs were respectively 0.41 and 0.24 during the NHP and HP. The NORs were respectively 0.15 and 0.22 during the NHP and HP. The NHP met the condition of a strong photochemical oxidation reaction (SOR > 0.25 and NOR > 0.1) (Khoder, 2002), indicating that most SO_4^{2-} and NO_3^- were formed through the photochemical oxidation of SO_2 and NO_2, respectively. The SOR during the NHP was higher than that during the HP, indicating that the more crucial role of secondary SO_4^{2-} during the NHP. NOR during the HP was slightly higher than that during the NHP; this was mainly affected by temperature because NH_4NO_3 decomposes in high temperature conditions, which results in decreased NO_3^- in particulate matter (Liu *et al.*, 2011). The SOR and NOR were lower during the HP than during the NHP; however, the effect of the secondary transformation on particles during the HP cannot be ignored.

Carbonaceous Aerosols Estimation from Biomass Burning

Crop residue burning can be expected to greatly contribute to carbonaceous aerosols during the HP, and the contribution can be estimated from the relationship between K^+ and OC, which are crucial components of biomass burning. K^+ has other sources (including sea salt, combustion, and industrial emissions); regarding reducing the effects of other sources of K^+, Pachon *et al.* (2013) developed a method for estimating K^+ from biomass burning on the basis of regression analysis between K^+ and other species that share sources with K^+, except biomass burning. The formula for estimating K^+ from biomass burning is as follows (Pachon *et al.*, 2013):

$$K^+_{biomass\ burning} = K^+ - 0.37 \times [Fe] \quad (3)$$

where $K^+_{biomass\ burning}$ represents the concentration of K^+ ion from biomass burning, K^+ represents the K^+ ion concentration, and [Fe] represents the Fe concentration (Pachon *et al.*, 2013).

$K^+_{biomass\ burning}$ during the HP was 1.72 μg m^{-3}, which 3.0-fold higher than that during the NHP, suggesting a higher contribution of biomass burning during the HP. Fig. 5 shows the correlation between $K^+_{biomass\ burning}$ and OC during the NHP and HP, and their respective correlation factors (Person's R) were 0.56 and 0.74. The strong correlation during the HP indicated biomass burning to be a vital source of OC.

The following equation can roughly calculate the percentage of OC contributed by biomass burning (Zheng *et al.*, 2005b):

$$OC\% = 100\% \times [(OC/K^+_{biomass\ burning})_{slope} \times K^+_{biomass\ burning}]/OC \quad (4)$$

Biomass burning yielded a 58% OC concentration during the HP.

CONCLUSIONS

In this study, $PM_{2.5}$ samples were collected, and online datasets (SO_2, NO_2, O_3, CO, PM_{10} and $PM_{2.5}$) were monitor for August 13–22 and October 21–31 in 2014. The chemical

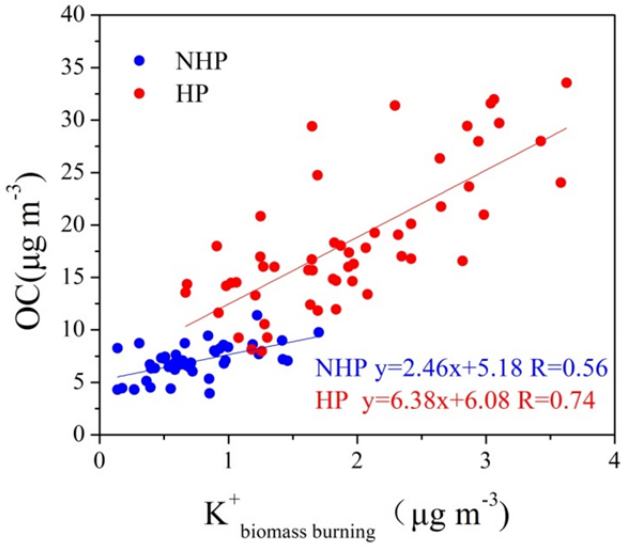

Fig. 5. Correlation between OC and $K^+_{biomass\ burning}$ during the NHP and HP.

components in the samples were analysed to determine differences in pollutant characteristics between the NHP and HP. The mass concentrations of particles and gaseous pollutants, except for O_3, were higher during the HP than during the NHP.

Compared with the mass concentrations of OC, Cl^-, NO_3^- and K^+ during the NHP, those during the NHP were significantly increased, and the mass fractions of OC, EC, Cl^- and K^+ during the HP were respectively 1.6, 1.3, 3.2, and 1.3-fold higher than those during the NHP. SO_4^{2-}, NO_3^-, and OC were the major chemical components of $PM_{2.5}$ during the HP. Biomass burning and secondary transformation may be concluded as being two major sources of $PM_{2.5}$ during the HP. Crop residues have varying K^+/Cl^- values, and the proportion of K^+ was lower than that of Cl^- in $PM_{2.5}$ from crop residue burning, indicating the presence of maize straw crop residues in the study area.

NH_4^+ and SO_4^{2-} respectively existed in $(NH_4)_2SO_4$ and NH_4HSO_4 forms, during the HP and NHP. Although the SORs and NORs were lower during the HP (respectively 0.24 and 0.15) than during the NHP (respectively 0.41 and 0.22), the effects of secondary transformations on particles during the HP cannot be ignored. Biomass burning yielded a 58% OC contribution during the HP.

ACKNOWLEDGMENTS

Danni Liang was supported in part by the Major State Research Development Program of China (2016YFC0208500). The authors thank the Heze Environmental Protection Administration for supporting the sampling and monitoring campaign.

DISCLAIMER

The authors have no connections to any companies or specific commercial products.

REFERENCES

Andreae, M.O. and Merlet, P. (2001). Emission of trace gases and aerosols from biomass burning. *Global Biogeochem. Cycles* 15: 955–966.

Cao, G.L., Zhang, X.Y., Wang, Y.Q. and Zheng, F.C. (2008). Estimation of emissions from field burning of crop straw in China. *Chin. Sci. Bull.* 53: 784–790.

Cheng, Y., Engling, G., He, K.B., Duan, F.K., Ma, Y.L., Du, Z.Y., Liu, J.M., Zheng, M. and Weber, R.J. (2013). Biomass burning contribution to Beijing aerosol. *Atmos. Chem. Phys.* 13: 7765–7781.

Cheng, Z., Wang, S., Fu, X., Watson, J.G., Jiang, J., Fu, Q., Chen, C., Xu, B., Yu, J., Chow, J.C. and Hao, J. (2014). Impact of biomass burning on haze pollution in Yangtze River Delta, China: A case study in summer 2011. *Atmos. Chem. Phys.* 14: 4573–4585.

Cui, H.Y., Chen, W.H., Dai, W., Liu, H., Wang, X.M. and He, K.B. (2015). Source apportionment of $PM_{2.5}$ in Guangzhou combining observation data analysis and chemical transport model simulation. *Atmos. Environ.* 16: 262–271.

Deng, L.Q., Li, H., Chai, F.H, Lun, X.X., Chen, Y.Z., Zhang, X.M. and Wang F.W. (2010). Pollution characteristics of the atmospheric fine particles and related gaseous pollutants in the northeastern urban area of Beijing in winter season. *China Environ. Sci.* 30: 954–961.

Dockery, D.G., Pope, C.A., Xu, X.P., Spengler, J.D., Ware, J.H., Fay, M.E., Ferris, B.G. and Speizer, F.E. (1993). An association between air–pollution and mortality in 6 United–States cities. *N. Engl. J. Med.* 329: 1753–1759.

Duan, F.K., Liu, X.D., Lu, Y.Q., Wang, L. and He, K.B. (2003). Concentration level of TSP and chemical speciation of ion species in Beijing. *Environ. Monit. China* 19: 13–17.

Duan, J.C. and Tan, J.H. (2013). Atmospheric heavy metals and Arsenic in China: Situation, sources and control policies. *Atmos. Environ.* 74: 93–101.

Eliana, P., Stefania, S., Andrea, L., Flavia, V. and Giancarlo, R. (2014). Secondary inorganic aerosol evaluation: Application of a transport chemical model in the eastern part of the Po Valley. *Atmos. Environ.* 98: 202–213.

Grosjean, D. and Friedlander, S.K. (1975). Gas-particle distribution factors for organic and other pollutants in the Los Angeles atmosphere. *J. Air Pollut. Control Assoc.* 25: 1038–1044.

Grosjean, D. and Seinfeld, J.H. (1989). Parameterization of the formation potential of secondary organic aerosols. *Atmos. Environ.* 23: 1733–1747.

Hays, M.D., Fine, P.M., Geron, C.D., Kleeman, M.J. and Gullett, B.K. (2008). Impact of biomass combustion on urban fine particulate matter in central and northern Europe. *Atmos. Environ.* 191: 265–277.

Haywood, J., Bush, M., Abel, S., Claxton, B., Coe, H., Crosier, J., Harrison, M., Macpherson, B., Naylor, M. and Osborne, S. (2008). Prediction of visibility and aerosol within the operational Met Office Unified Model II: Validation of model performance using observational

data. *Q. J. R. Meteorolog. Soc.* 134: 1817–1832.

Hong, Z., Chak, K.C., Ming, F. and Anthony, S.W. (1999). Size distributions of particulate sulfate, nitrate, and ammonium at a coastal site in Hong Kong. *Atmos. Environ.* 33: 843–853.

Hu, M., Tang, Q., Peng, J.F., Wang, E.Y., Wang, S.L. and Chai, F.H. (2011). Study on characterization and source apportionment of atmospheric particulate matter in China. *Environ. Sustainable Dev.* 5: 15–19.

Hu, Z.M., Wang, J., Chen, Y.Y., Chen, Z.L. and Xu, S.Y. (2014). Concentrations and source apportionment of particulate matter in different functional areas of Shanghai, China. *Atmos. Pollut. Res.* 5: 138–144.

Huang, K., Fu, J.S., Hsu, N.C., Gao, Y., Dong, X., Tsay, Y.F. and Lam, Y.F. (2013). Impact assessment of biomass burning on air quality in Southeast and East Asia during BASE-ASIA. *Atmos. Environ.* 78: 291–302.

Jain, N., Bhatia, A. and Pathak, H. (2014). Emission of air pollutants from crop residue burning in India. *Aerosol Air Qual. Res.* 14: 422–430.

Kadowaki, S. (1986). On the nature of atmospheric oxidation processes of SO_2 to sulfate and of NO_2 to nitrate on the basis of diurnal variations of sulfate, nitrate, and other pollutants in an urban area. *Environ. Sci. Technol.* 20: 1249–1253.

Khoder, M.I. (2002). Atmospheric conversion of sulphur dioxide to particulate sulfate and nitrogen dioxide to particulate nitrate and gaseous nitric acid in an urban area. *Chemosphere* 49: 675–684.

Lestari, P. and Mauliadi, Y.D. (2009). Source apportionment of particulate matter at urban mixed site in Indonesia using PMF. *Atmos. Environ.* 43: 1760–1770.

Li, J.F., Song, Y., Mao, Y., Mao, Z.C., Wu, Y.S., Li, M.M., Huang, X., He, Q.C. and Hu, M. (2014). Chemical characteristics and source apportionment of $PM_{2.5}$ during the harvest season in eastern China's agricultural regions. *Atmos. Environ.* 92: 442–448.

Li, X.G., Wang, S.X., Duan, L., Hao, J., Li, C., Chen, Y.S. and Yang, L. (2007). Particulate and trace gas emissions from open burning of wheat straw and corn stover in China. *Environ. Sci. Technol.* 41: 6052–6058.

Lin, P., Engling, G. and Yu, J.Z. (2010). Humic–like substances in fresh emissions of rice straw burning and in ambient aerosols in the Pearl River Delta Region, China. *Atmos. Chem. Phys.* 10: 6487–6500.

Liu, S., Hu, M., Slanina, S., He, L.Y., Niu, Y.W., Bruegemann, E., Gnauk, T. and Herrmann, H. (2008). Size distribution and source analysis of ionic compositions of aerosols in polluted periods at Xinken in Pearl River Delta (PRD) of China. *Atmos. Environ.* 42: 6284–6295.

Liu, Z.R., Wang, Y.S., Liu, Q., Liu, L.N. and Zhang, D.Q. (2011). Pollution characteristics and source of the atmospheric fine particles and secondary inorganic compounds at Mount Dinghu in autumn season. *Environ. Sci.* 32: 3160–3166.

Liu, Z.R., Hu, B., Liu, Q., Sun, Y. and Wang, Y.S. (2014). Source apportionment of urban fine particle number concentration during summertime in Beijing. *Atmos. Environ.* 96: 359–369.

Luo, Z.X., Gao, M.R., Luo, X.S. and Yan, C.Z. (2016). National pattern for heavy metal contamination of topsoil in remote farmland impacted by haze pollution in China. *Atmos. Res.* 170: 34–40.

Mather, T., Allen, A., Oppenheimer, C., Pyle, D. and McGonigle, A.J.S. (2003). Size-resolved characterisation of soluble ions in the particles in the tropospheric plume of Masaya volcano, Nicaragua: Origins and plume processing. *J. Atmos. Chem.* 46: 207–237.

Ohta, D. and Okita, D. (1990). A chemical characterization of atmospheric aerosol in Sapporo. *Atmos. Environ.* 24: 815–822.

Possanzini, M., Santis, F.D. and Palo, V.D. (1999). Measurements of nitric acid and ammonium salts in lower Bavaria. *Atmos. Environ.* 33: 3597–3602.

Sillapapiromsuk, S., Chantara, S., Tengjaroenkul, U., Prasitwattanaseree, U. and Prapamontol, U. (2013). Determination of PM_{10} and its ion composition emitted from biomass burning in the chamber for estimation of open burning emissions. *Chemosphere* 93: 1012–1019.

Song, Y., Zhang, Y.H., Xie, S.D., Zeng, L.M., Zheng, M., Lynn, G., Salmon, Shao, M., Sjaak and Slanina. (2006). Source apportionment of $PM_{2.5}$ in Beijing by positive matrix factorization. *Atmos. Environ.* 40: 1526–1537.

Streets, D.G., Yarber, K.F., Woo, J.H. and Carmichael, G.R. (2003). Biomass burning in Asia: Annual and seasonal estimates and atmospheric emissions. *Global Biogeochem. Cycles* 17: 1099–1118.

Sun, Y.L., Wang, Z.F., Wild, O., Xu, W.Q., Chen, C., Fu, P.Q., Du, W., Zhou, L.B., Zhang, Q., Han, T.T., Wang, Q.Q., Pang, X.L., Zheng, H.T., Li, J., Guo, X.F., Liu, J.G. and Worsnop, D.R. (2016). "APEC Blue" secondary aerosol reductions from emission controls in Beijing. *Sci. Rep.* 2: 1–9.

Turn, S.Q., Jenkins, B. M., Chow, J.C., Pritchett, L.C., Campbell, D., Cahill, T. and Whalen, S.A. (1997). Elemental characterization of particulate matter emitted from biomass burning: Wind tunnel derived source profiles for herbaceous and wood fuels. *J. Geophys. Res.* 102: 3683–3699.

Wang, H.L, Zhu, B., Shen, L.J., Xu, H.H., An, J.L., Xue, G.Q. and Cao, X.F. (2015). Water-soluble ions in atmospheric aerosols measured in five sites in the Yangtze River Delta, China: Size-fractionated, seasonal variations and sources. *Atmos. Environ.* 123: 370–390.

Wang, X.F., Wang, W.X., Yang, L.X., Gao, X.M., Nie, W., Yu, Y.C., Xu, P.J., Zhou, Y. and Wang, Z. (2012). The secondary formation of inorganic aerosols in the droplet mode through heterogeneous aqueous reactions under haze conditions. *Atmos. Environ.* 63: 68–76.

Wang, Y.J., Hu, M., Wang, Y., Qin, Y.H., Chen, H.Y., Zeng, L.M., Lei, J.R., Huang, X.F., He, L.Y., Zhang, R.Q. and Wu, Z.J. (2016). Characterization and influence factors of $PM_{2.5}$ emitted from crop straw burning. *Acta Chim. Sinica* 74: 356–362.

Watson, J.G. (2002). Visibility: Science and regulation. *J. Air Waste Manage. Assoc.* 52: 628–713.

Wen, T.X., Wang, Y.S. and Zhang, K. (2007). Study on sulfate and sulphur oxidation ratio in PM_{10} during heating

season in Beijing. *J. Univ. Chin. Acad. Sci.* 24: 584–589.

Yuan, C.S., Lee, C.G. and Liu, S.H. (2006). Correlation of atmospheric visibility with chemical composition of Kaohsiung aerosol. *Atmos. Res.* 82: 663–679.

Zhang, H.F., Hu, J., Qi, Y.X., Li, C.L., Chen, J.M., Wang, X.M., He, J.W., Wang, S.X., Hao, J.M., Zhang, L.L., Zhang, L.J., Zhang, Y.X., Li, R.K., Wang, S.L. and Chai, F.H. (2017). Emission characterization, environmental impact, and control measure of $PM_{2.5}$ emitted from agricultural crop residue burning in China. *J. Cleaner Prod.* 149: 629–635.

Zhang, T.R., Wooster, M.J., Green, D.C. and Main, B. (2015). New field-based agricultural biomass burning trace gas, $PM_{2.5}$, and black carbon emission ratios and factors measured *in situ* at crop residue fires in Eastern China. *Atmos. Environ.* 121: 22–34.

Zhang, Z.L., Wang, J., Chen, L.H. and Lu, W.J. (2013). Impact of haze and air pollution-related hazards on hospital admissions in Guangzhou. *Environ. Sci. Pollut. Res.* 21: 4236–4244.

Zheng, M., Salmon, L.G., Schauer, J.J., Zeng, L., Kiang, C.S., Zhang, Y. and Cass, G.R. (2005a). Seasonal trends in $PM_{2.5}$ source contributions in Beijing, China. *Atmos. Environ.* 39: 3967–3976.

Zheng, X., Liu, X., Zhao, H., Duan, F., Yu, T. and Cachier, H. (2005b). Seasonal characterization of biomass burning contribution in airborne particles in Beijing. *Sci. China Ser. B Chem.* 35: 346–352.

Zheng, M., Zhang, Y.J., Yan, C.Q., Zhu, X.L., James, J.S. and Zhang, Y.H. (2014). Review of $PM_{2.5}$ source apportionment methods in China. *Acta Sci. Natur. Univ. Pekinensis.* 50: 1141–1154.

Received for review, September 5, 2016
Revised, April 28, 2017
Accepted, April 28, 2017